

Article

Test and Evaluation of the Flexural Properties of Reinforced Concrete Beams with 100% Recycled Coarse Aggregate and Manufactured Sand

Changyong Li ^{1,2} , Tongsheng Liu ¹, Hao Fu ¹, Xiaoyan Zhang ¹, Yabin Yang ¹ and Shunbo Zhao ^{1,2,*} 

- ¹ International Joint Research Lab for Eco-Building Materials and Engineering of Henan, School of Civil Engineering and Communications, North China University of Water Resources and Electric Power, Zhengzhou 450045, China; lichang@ncwu.edu.cn (C.L.); x201910306241@stu.ncwu.edu.cn (T.L.); Z20201030386@stu.ncwu.edu.cn (H.F.); zxyanzi@ncwu.edu.cn (X.Z.); yangyabin@ncwu.edu.cn (Y.Y.)
- ² Collaborative Innovation Center for Efficient Utilization of Water Resources, North China University of Water Resources and Electric Power, Zhengzhou 450045, China
- * Correspondence: sbzhao@ncwu.edu.cn; Tel.: +86-371-69127378

Abstract: Although studies have been performed on the recycled aggregate made of waste concrete for the production of new concrete, the new concrete with 100% recycled coarse aggregate and manufactured sand (abbreviated as RAMC) still needs to be researched for structural applications. In this paper, an experimental study was performed on seven groups, including fourteen reinforced RAMC beams under the simply supported four-point loading test, considering the factors of the strength of RAMC and the reinforcement ratio of longitudinal tensile rebars. Based on the test results, the cracking resistance, the bearing capacity, the crack width, the flexural stiffness and the mid-span deflection of reinforced RAMC beams in bending are discussed and examined by using the formulas of conventional reinforced concrete beams. Results show that an obvious effect of reinforcement ratio was present, while less so was that of the strength of RAMC. With the comparison of predicted values by the formulas of conventional reinforced concrete beams, the reinforced RAMC beams decreased cracking resistance by about 20%, increased crack width by about 15% and increased mid-span deflection by about 10%, although the same bearing capacity can be reached. The results directly relate to the lower tensile strength of RAMC which should be further improved.

Keywords: beam; concrete; recycled coarse aggregate; manufactured sand; cracking resistance; crack width; deflection; bearing capacity



Citation: Li, C.; Liu, T.; Fu, H.; Zhang, X.; Yang, Y.; Zhao, S. Test and Evaluation of the Flexural Properties of Reinforced Concrete Beams with 100% Recycled Coarse Aggregate and Manufactured Sand. *Buildings* **2021**, *11*, 420. <https://doi.org/10.3390/buildings11090420>

Academic Editors: Binsheng (Ben) Zhang and Wei (David) Dong

Received: 21 August 2021
Accepted: 12 September 2021
Published: 19 September 2021

Publisher's Note: MDPI stays neutral with regard to jurisdictional claims in published maps and institutional affiliations.



Copyright: © 2021 by the authors. Licensee MDPI, Basel, Switzerland. This article is an open access article distributed under the terms and conditions of the Creative Commons Attribution (CC BY) license (<https://creativecommons.org/licenses/by/4.0/>).

1. Introduction

Solid wastes from construction of urban and other infrastructures need to be urgently recycled to eliminate secondary pollution in the abandonment process and protect the environment. This promotes the recycling of aggregate made from demolished waste concrete for the production of new concrete [1,2]. Meanwhile, with the requirement of protection for farmland and river courses, manufactured sand becomes a common fine aggregate of concrete [3,4]. Therefore, the conventional concrete made of natural aggregates calls for a fundamental change to be produced with recycled aggregates and manufactured sand.

Many studies have been performed on the properties of concrete with recycled aggregate and/or manufactured sand at the materials level, with a view to ensure the equivalent properties of conventional concrete or determine the difference from conventional concrete [2,4–6]. Several kinds of methods have been tried to overcome the defects of recycled aggregate, such as rough surface bonded to old cement mortar, low density with high porosity and quick water absorption [7–9]. Most studies have been done on the concrete

produced by replacing natural aggregate with recycled aggregate. The effects of the replacement ratio were mainly confirmed on the basic mechanical properties of concrete and the loading performances of reinforced concrete structural members such as beams in bending and shear. Results indicate that, compared to conventional concrete, and owing to defects of recycled coarse aggregate, the tensile strength and the modulus of elasticity of recycled aggregate concrete decreased with the increase in the replacement ratio [2,5,8–10]. The bond strength of steel bar in recycled aggregate concrete decreased by about 13–21% with the increase in replacement ratio, and there was a strong relation with the crushing strength of recycled coarse aggregate [11,12]. This gave the reinforced recycled aggregate concrete beams increased crack width and deflection, compared to the conventional reinforced concrete beams [13–15]. One of the effective measures to improve the loading behaviors is to employ steel fiber [16–18].

In view of the performance of concrete obviously affected by the weakened interface of recycled coarse aggregate to binder paste [9,10], a technology of composite aggregate with recycled aggregate and natural aggregate was proposed. The composite aggregate consists of small particles of recycled coarse aggregate and large particles of natural aggregate in proper proportions to meet the continuous particle grading. Satisfactory strength of concrete and reliable loading performance of reinforced concrete beams can be provided by using the composite recycled aggregate [19–21]. Another attempt was to produce concrete with 100% recycled coarse aggregate and manufactured sand (abbreviated as RAMC). This method intends to add the benefits of the stone powder of manufactured sand to the microstructure of concrete. The benefits include the micro-aggregate filling effect on density, the activity effect and crystal nuclei effect on cement hydration, and the enhancement effect on the interface of the aggregate to set cement [4,22,23]. This gives the concrete satisfactory performances in terms of good workability of fresh mix, reasonable basic mechanical properties with long-term development and acceptable durability for the structural application [24–26]. As a result, the RAMC presents good basic mechanical properties except for a slightly lower tensile strength than predicted [27]. This encourages the research of RAMC for structural application. Under this condition, solid wastes recycling for the production of new concrete can reach a high level with 100% recycled coarse aggregate and manufactured sand.

Therefore, based on the loading mechanism of reinforced concrete beams, in this paper, a study was carried out on the bending performance of reinforced RAMC beams. Considering the main factors of the reinforcement ratio of longitudinal tensile rebars and the strength of RAMC, seven groups with fourteen test beams were prepared and experimentally studied by using the simple supported four-point loading test. The cracking load, ultimate load, crack distribution and development, crack width and deflection were measured. Test results are compared to the results predicted by formulas specified in current design codes for conventional reinforced concrete beams, the differences and similarities are discussed in detail as they inhere in the combination of the features of RAMC and the bond performance of rebars and revisions are proposed for the correct prediction of reinforced RAMC beam.

2. Materials and Methods

2.1. Preparation of RAMC

Ordinary Portland cement of grade 42.5 produced by Jiaozuo Jiangu Cement Co. Ltd. was used; the chemical components are presented in Table 1. This met the specifications of China code GB175 [28].

Table 1. Physical and mechanical properties of cement.

Setting Time (min)		Compressive Strength (MPa)		Flexural Strength (MPa)		Fineness (%)	Water Requirement of Normal Consistency (%)	Apparent Density (kg/m ³)
Initial	Final	3d	28d	3d	28d			
180	285	33.3	53.5	5.7	9.2	9.2	29.0	3110

The coarse recycled aggregate was made from waste concrete. It consisted of series of 5–10, 10–20 and 20–25mm with a proportion of 4:3:3 to form a continuous grading of particles according to the specification of China code GB/T240 [1]. The apparent density and the closed-packing density were 2650 and 1460 kg/m³; the 1 h water absorption was 4.55% and the crushed index was 24.8%.

The manufactured sand used was with a fineness modulus of 3.13 and a water absorption of 0.90%. The mix water was tap water. A high-performance water reducer was used.

The mix proportions of RAMCs with strength grade of 30, 40 and 50 MPa were designed by using the absolute volume method [27]. The results of mix proportion of RAMCs are presented in Table 2. As the design was made on the premise of saturated aggregates at the surface drying condition, additive water was considered in view of the 1 h water absorption of recycled coarse aggregate. The sand ratio was adjusted to get a rational workability of fresh mix [4]. According to the design of test beams in this study, one batch of RAMC with a strength grade of 30 MPa was made with a slump of 65 mm, three batches of RAMC with a strength grade of 40 MPa were made with a slump around 100 mm, and one batch of RAMC with a strength grade of 50 MPa was made with a slump of 105 mm.

Table 2. Results of mix proportion of RAMC.

Strength Grade (MPa)	w/c	Raw Material Dosage (kg/m ³)					Sand Ratio	
		Cement	Water	Manufacture Sand	Recycled Coarse Aggregate	Additive Water		Water Reducer
30	0.55	300.0	165	864.2	1081.1	51.9	1.49	0.44
40	0.45	366.7	165	820.7	1086.2	51.5	1.83	0.42
50	0.36	458.3	165	657.4	1148.8	52.5	2.28	0.36

A horizontal-shaft forcing mixer was used. Recycled coarse aggregate and manufactured sand were mixed with the additive water for 2 min. Then other raw materials were added and mixed for 3 min. For each batch of RAMC, six cubic specimens, three as a group, with a dimension of 150 mm were formed for the test of the cubic compressive strength (f_{cu}) and splitting tensile strength (f_t); six prism specimens, three as a group, with a dimension of 150 × 150 × 300 mm were formed for the test of the axial compressive strength (f_c) and modulus of elasticity (E_c). All specimens were cured in the same condition of test beams. The test results are presented in Table 3.

Table 3. Test results of cross section, RAMC properties and reinforcement of test beams.

Beam No.	Dimension (mm)		Properties of RAMC				Longitudinal Tensile Rebars Number × d (mm)	Cross-Section Area A_s (mm ²)	Reinforcement Ratio ρ (%)
	b	h	f_{cu} (MPa)	f_c (MPa)	f_t (MPa)	E_c (GPa)			
RC3-0.93	154	401	46.0	40.0	2.40	30.2	2 × 18	509	0.90
RC4-0.41	150	400	55.0	43.5	2.57	32.5	2 × 12	226	0.41
RC4-0.93	153	403	53.7	41.9	2.60	32.4	2 × 18	509	0.90
RC4-1.40	157	401	55.0	43.5	2.57	32.5	2 × 22	760	1.33
RC4-1.81	155	402	53.7	41.9	2.60	32.4	2 × 25	982	1.74
RC4-3.47	158	402	52.4	42.6	2.45	32.6	2 × 22 + 2 × 25	1724	3.21
RC5-0.93	153	403	61.3	58.7	3.00	33.7	2 × 18	509	0.90

2.2. Preparation of Test Beams

Hot-rolled deformed steel bar was used for the longitudinal tensile rebars with a diameter of 12, 18, 22 and 25 mm, respectively. The test results of the yield strength (f_y) corresponded to 420, 390, 390 and 375 MPa, respectively. The modulus of elasticity (E_s) corresponded to 202, 201, 205 and 202 GPa, respectively. Hot-rolled plain steel bar with

a diameter of 10 mm was used for the longitudinal construction rebars, and that with a diameter of 8 mm was used for the stirrups.

Considering the factors of RAMC strength and reinforcement ratio, seven groups of test beams were designed. Each group included two beams with the same condition based on the specification of China code GB/T50152 [29]. The length of beams was 3500 mm. The rectangular section was of a width $b = 150$ mm and a depth $h = 400$ mm.

The beams were designed to fail in bending with a proper longitudinal tensile reinforcement. The sufficient stirrups were placed to ensure the shear capacity at shear-span of the test beams. Five ratios of the longitudinal tensile reinforcement were selected from 0.41 to 3.47% within the limit of conventional reinforced concrete beams specified in the China code GB 50010 [30]. Details of the placement of the steel bars are presented in Figure 1; the span of the test beam was 3200 mm with a shear-span of 850 mm and a pure bending part of 1500 mm. The thickness of concrete cover for the longitudinal steel bars was 25 mm. The steel formwork was used for the cast of test beams, and was demolded after being cured for 24 h. Then the beams were cured with spraying water for 7 days, and were placed in the natural condition further for about 21 days before testing.

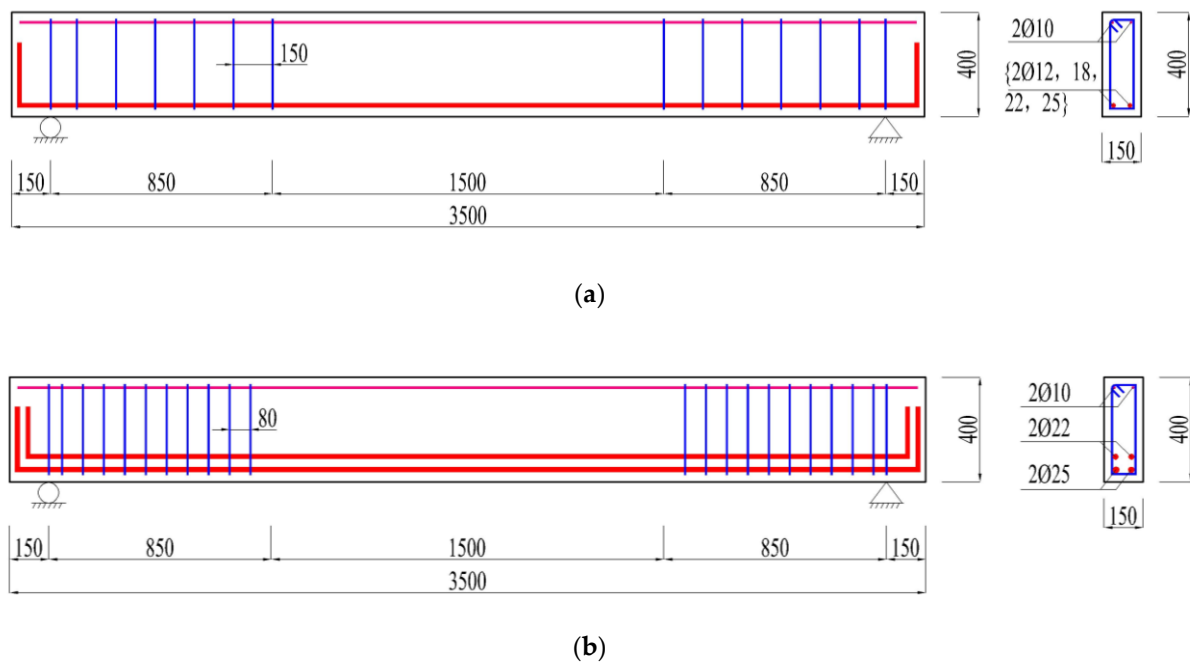


Figure 1. Details of test beams: (a) with single row of rebars; (b) with two rows of rebars; (Unit: mm).

2.3. Loading Method and Measurements

Tests were carried out by the simply supported under four-point loading test method according to the specification of China standard GB50152 [29]. As presented in Figure 2, the loading device consisted of the steel frame, hydraulic jack and load sensors. The columns of the steel frame were fixed to the foundation of the testbed. Two hydraulic jacks symmetrically exerted the concentrated loads step by step on the top surface of the test beams. The load sensors were used to control the load of each step. Three strain gauges were pasted on the top surface of pure bending part to measure the compressive strains of RAMC, and another strain gauge and two dial strain gauges were pasted on the side surface of mid-span section to measure the strain distribution along the sectional depth. Five electrical displacement meters were installed at the mid-span, the loading sections and the supports to measure the mid-span deflection. The test data were collected by a data acquisition system.

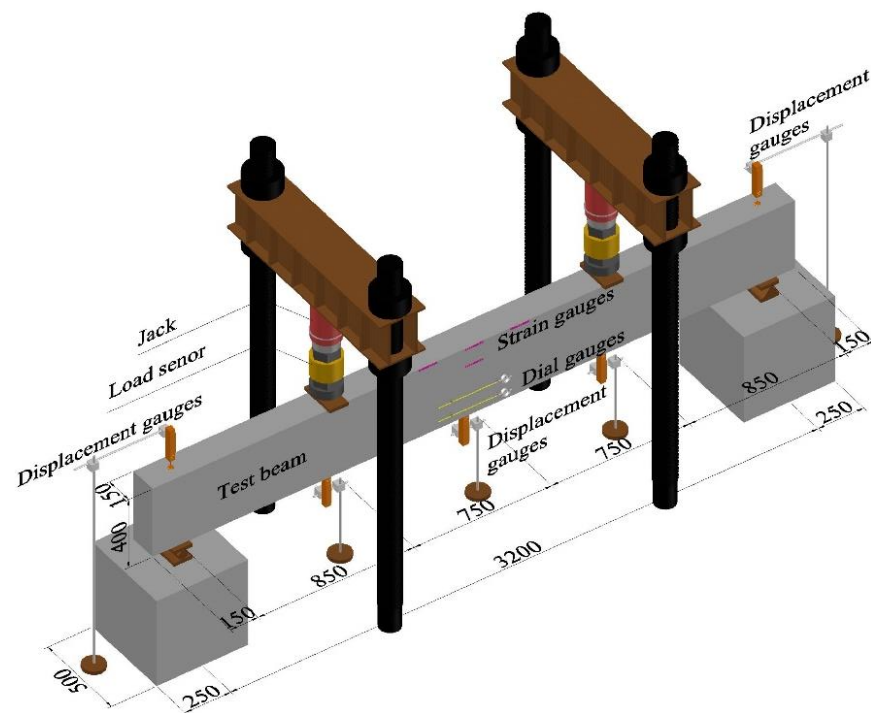


Figure 2. Test loading device and arrangement of measurements (Unit: mm).

The load of each step was about 10% of the predicted ultimate load. When the load closed to the cracking resistance and the ultimate, the load of each step was decreased to 5% of the predicted ultimate load. The load corresponding to RAMC cracking in bending was determined considering the first crack(s) appeared on the side surface of the test beam at the barycenter of the longitudinal tensile rebars, and the first point with changed slope at the load-deflection curve. The appearance and developing process of cracks were recorded on the sides of the test beams with the loading process. The crack width was detected by the electrical reading microscope with a 0.02 mm precision on the side surfaces at the barycenter of the longitudinal tensile rebar.

3. Test Results and Discussion

3.1. Bearing Capacity

Similar to the conventional reinforced concrete beam, the strain of RAMC at different height of mid-span section were linear with the distance from the neutral axis. This indicates that the plane section hypothesis was also adaptable to the strain distribution at normal sections [31]. All test beams failed in bending with the yield of longitudinal tensile rebars after the process of elastic, cracking, yielding and failure. With the increase in the reinforcement ratio of longitudinal tensile rebars, the crushed depth became obvious due to the largely increased compressive strain of RAMC under the increasing load. The test beams with the reinforcement ratio of 3.47% failed in crushed RAMC in compression. Meanwhile, RAMC strength had a less effect on the bearing capacity of the test beams with a lower reinforcement ratio, as a less crushed depth of RAMC in compression was observed.

Referencing the design method for the bearing capacity of conventional reinforced concrete beams in flexure [30], the ultimate moment M_u of test beams can be predicted by formula as follows:

$$M_u = f_y A_s \left(h_0 - \frac{f_y A_s}{2 f_c b} \right) \quad (1)$$

where $h_0 = h - a_s$ is the effective depth of the normal section, and a_s is the distance of barycenter of longitudinal tensile rebars.

The test results of the ultimate moment computed by ultimate load multiplying shear-span are presented in Table 4. The ratio of the test results to the predicted results changes from 0.936 to 1.143. The average is 0.995 with a variation coefficient of 0.063. Therefore, the reinforced RAMC beams present with almost the same ultimate moment of the conventional reinforced concrete beams. This is due to the test beams failing with the yield of longitudinal tensile rebar on the premise of enough axial compressive strength of RAMC. In this study, the axial compressive strength f_c changed from 78.0 to 95.7% of the cubic compressive strength f_{cu} , as presented in Table 2. The average ratio of f_c/f_{cu} was 0.826 with a variation coefficient of 0.079. This satisfies the requirement $f_c/f_{cu} = 0.76$ for the conventional concrete [30].

Table 4. Test results of cracking and ultimate moments of test beams.

Beam No.	RC3-0.93	RC4-0.41	RC4-0.93	RC4-1.40	RC4-1.81	RC4-3.47	RC5-0.93
Ultimate moment M_u (kN·m)	69.8	32.4	68.1	98.7	120.8	218.6	69.0
Cracking moment M_{cr} (kN·m)	15.8	11.0	15.4	15.9	18.4	17.6	19.1
M_{cr}/M_u	0.23	0.34	0.23	0.16	0.15	0.08	0.27

3.2. Cracking Resistance

The simplified formula deduced from the Traditional Materials Mechanics is always applied to predict the cracking moment of reinforced concrete beams:

$$M_{cr} = \gamma_m f_t W_0 \quad (2)$$

where γ_m is the plastic coefficient of the sectional resistance moment; W_0 is the elastic resistance moment of transferred section to tensile edge.

Meanwhile, the test results are verified by the formulas specified in the China codes GB 50010, JTJ 220 and DL/T 5057 as follows [28,32,33]:

$$\gamma_m = 1.55(0.7 + \frac{120}{h}) \quad (3)$$

$$\gamma_m = 1.55(0.85 + \frac{50}{h}) \quad (4)$$

$$\gamma_m = 1.55(0.7 + \frac{300}{h}) \quad (5)$$

The formula considering the effects of reinforcement ratio and concrete cover is also used:

$$\gamma_m = 1.55\gamma_h\gamma_{c\rho} \quad (6)$$

In Formulas (4) and (5), taken $h = 750$ mm when $h < 750$ mm. In Formula (6), $\gamma_h = 0.73 + 50/h$, $\gamma_{c\rho} = 1.2 - (0.042c/d) + 5\rho$, taken $\rho = 2\%$ when $\rho > 2\%$. c is the thickness of concrete cover, d is the diameter of longitudinal tensile reinforcement.

The test results of the cracking moment computed by cracking load multiplying shear-span are presented in Table 4. The averages of the ratio of the test results to the predicted results by Formula (2) corresponding to Formulas (3), (4), (5) and (6) are 0.801, 0.874, 0.729 and 0.796, respectively, with a variation coefficient of 0.120. The ratio tends to increase with the tensile strength of RAMC and the reinforcement ratio. This indicates that the lower cracking resistance of test beams is about 20% lower than that of the conventional reinforced concrete beams [34].

In view of the above formulas, the lower cracking resistance can be mainly put down to a lower tensile strength of RAMC. By using the prediction Formula (7) of conventional concrete specified in the China code GB 50010 [30], the ratio of test results as presented in Table 3 to the predicted values varied from 0.703 to 0.789. The average was 0.734 with a variation coefficient of 0.038. The decreased percent of tensile strength basically coincided

with the decrease percent of cracking resistance of reinforced RAMC beams. Therefore, to improve the tensile strength of RAMC is the core to improve the cracking resistance of reinforced RAMC beams.

$$f_t = 0.395 f_{cu}^{0.55} \quad (7)$$

3.3. Cracking Distribution and Crack Width

As presented in Figure 3, for the crack distribution on the pure bending part of test beams, vertical cracks of RAMC under bending appeared successively on the side surfaces of test beams and extended continuously from bottom to top with the increasing load, except some short cracks became a dead state. When the load was about 80–90% of the ultimate, the main cracks diverged as the Y shape. This indicated that the neutral axis basically maintained constant with the continuously increasing load.

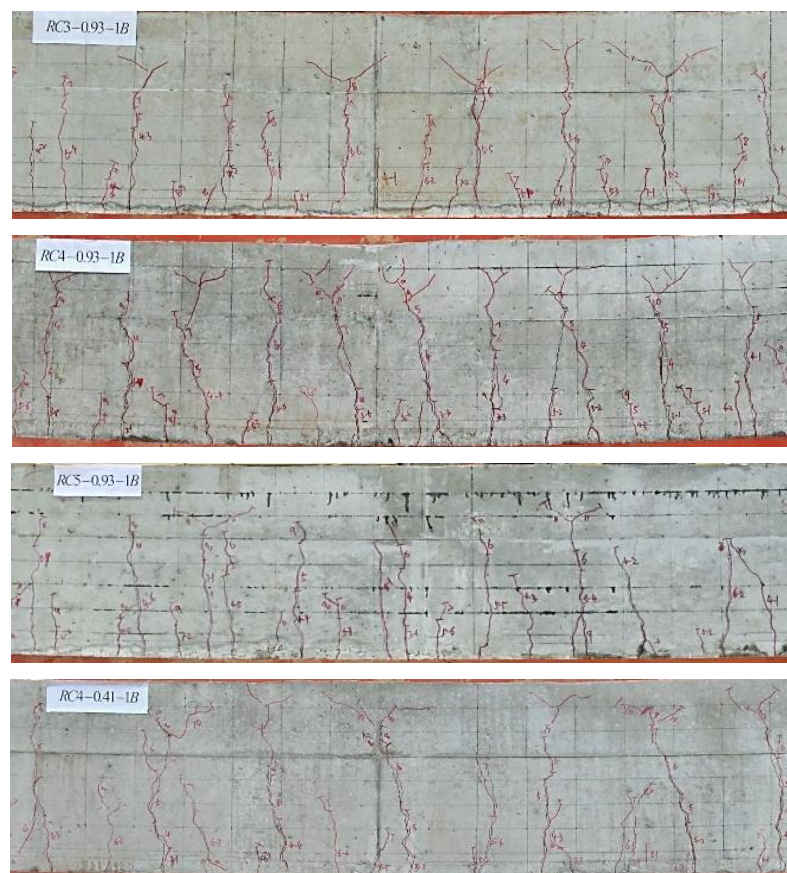


Figure 3. Cont.

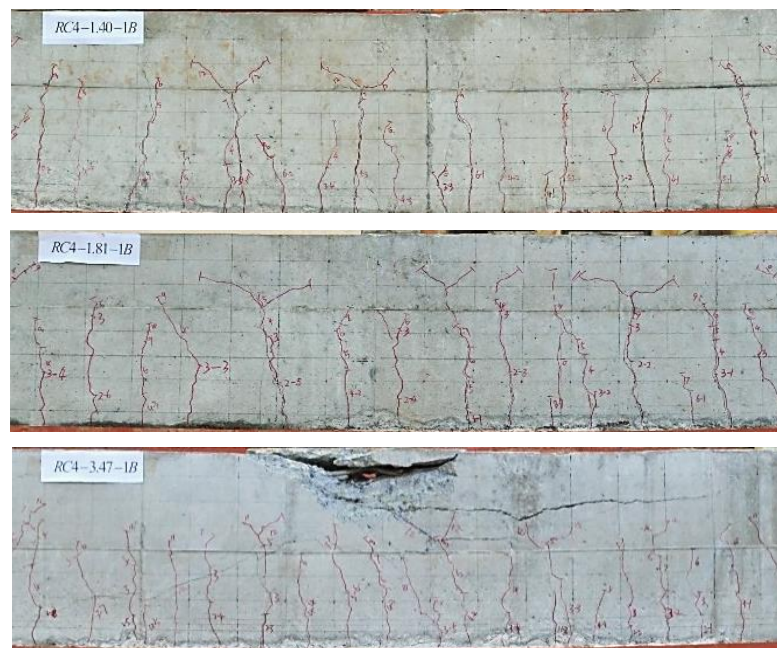


Figure 3. Cracks distribution on the pure bending part of test beams.

Based on the statistical principle of crack patterns, the cracks on test beams of this study were also divided into four types [35,36]. Only the cracks continuously developed with the increasing loads were considered as the main cracks. Other occasionally or randomly appeared cracks were not counted. In this study, the percent of main cracks in total cracks was 76.9%.

Referencing the formula of average crack spacing for the conventional reinforced concrete beams specified in the China code GB50010 [30], the coefficient related to the reinforcement is revised from 0.08 to 0.11, and the average crack spacing of test beams can be predicted as follows:

$$l_{cr} = 1.9c + 0.1 \frac{d}{\rho_{te}} \quad (8)$$

where l_{cr} is the average crack spacing; ρ_{te} is the effective reinforcement ratio of longitudinal tensile rebars, $\rho_{te} = A_s / (0.5bh)$. Taken $\rho_{te} = 0.01$ when $\rho_{te} < 0.01$.

The comparison of the test results with the computed values are presented in Figure 4. The fitness is better, the average ratio of the test results to the computed ones is 1.042 with a variation coefficient of 0.124. However, if the coefficient 0.1 of the second item in Formula (8) changed to 0.08 as specified in the China code GB 50,010 for the conventional reinforced concrete beams [30], the average ratio became 1.201 with a variation coefficient of 0.122. This indicates that the average crack spacing of reinforced RAMC beams increased by 15.9% compared to that of the conventional reinforced concrete beams. As the second item of Formula (8) mainly reflects the effect of longitudinal tensile rebars on the crack spacing, the bond behavior of rebar to RAMC plays a role in controlling it. As reported in previous studies, the bond strength of rebar in concrete decreases with the presence of recycled aggregate [11,12,37,38]. This leads to a need for a longer length to transfer the tensile stress between adjacent cracks along the bond interface between rebar and RAMC. As a result, the cracks form in a larger interval.

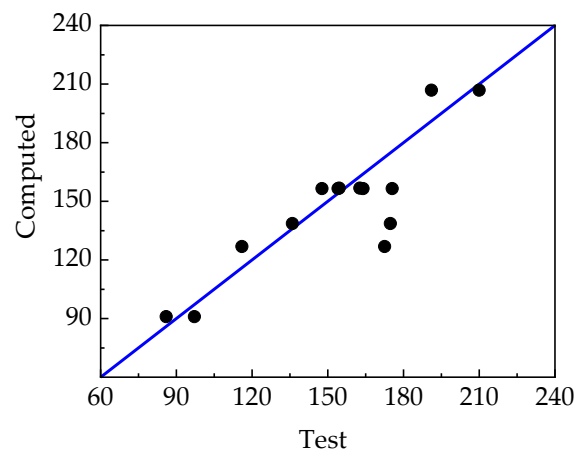


Figure 4. Comparison of test to computed results of crack spacing.

Due to the multiphase composite properties of concrete, the tensile stress was different in each section of the pure bending segment of test beams. This resulted in the cracks appearing randomly at the weaker section while the tensile stress of RAMC transferred unevenly along the longitudinal tensile rebars across cracks; the width of each crack varied. Therefore, a statistical analysis is needed to obtain the average crack width and the enlarged coefficient. The average crack width represents the distribution and extension level of cracks, and the enlarged coefficient represents the amplification of average width to the maximum width of crack with a statistical guarantee. Finally, the serviceability and durability of structures relate to the maximum crack width [30,39,40].

For the test beams at the normal service stage of loading level M/M_u at about 0.45–0.75, the test values of the average and maximum crack widths are presented in Table 5.

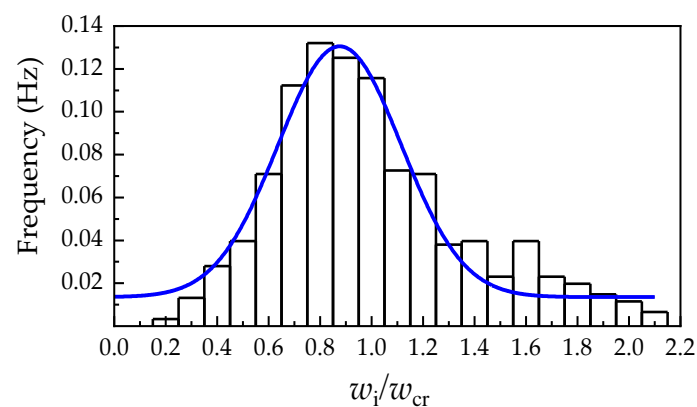
Table 5. Test data of crack widths and mid-span deflections of test beams.

Beam No.	Moment M (kN·m)	Moment Ratio M/M_u	Average Crack Width w_{cr} (mm)	Maximum Crack Width w_{max} (mm)	Mid-Span Deflection a_f (mm)
RC3-0.93-1	36.3	0.52	0.09	0.16	4.65
	45.0	0.65	0.14	0.23	6.05
	51.9	0.74	0.16	0.26	7.14
RC3-0.93-2	36.3	0.52	0.09	0.16	4.87
	43.2	0.62	0.13	0.23	6.08
	49.8	0.71	0.15	0.24	7.29
RC4-0.41-1	18.2	0.56	0.06	0.10	2.93
	21.6	0.67	0.09	0.16	4.22
	24.9	0.77	0.12	0.19	5.07
RC4-0.41-2	18.1	0.56	0.05	0.09	2.68
	21.4	0.66	0.08	0.14	3.90
	23.7	0.73	0.11	0.19	4.71
RC4-0.93-1	34.8	0.51	0.07	0.10	4.23
	41.6	0.61	0.10	0.17	5.26
	49.8	0.73	0.12	0.20	6.23
RC4-0.93-2	35.1	0.52	0.06	0.12	4.08
	42.3	0.62	0.09	0.18	5.32
	49.0	0.72	0.12	0.22	6.62
	52.8	0.77	0.13	0.25	7.43

Table 5. Cont.

Beam No.	Moment M (kN·m)	Moment Ratio M/M_u	Average Crack Width w_{cr} (mm)	Maximum Crack Width w_{max} (mm)	Mid-Span Deflection a_f (mm)
RC4-1.40-1	53.2	0.54	0.08	0.13	5.19
	62.7	0.64	0.10	0.18	6.19
	71.4	0.72	0.12	0.20	7.21
RC4-1.40-2	50.7	0.51	0.06	0.11	4.33
	61.9	0.63	0.09	0.17	5.49
	71.7	0.73	0.13	0.22	7.27
RC4-1.81-1	50.3	0.42	0.07	0.12	5.48
	62.4	0.52	0.10	0.15	6.82
	74.1	0.61	0.12	0.19	8.24
RC4-1.81-2	68.1	0.56	0.08	0.14	5.93
	80.0	0.66	0.10	0.17	7.20
	92.2	0.76	0.13	0.22	8.49
RC4-3.47-1	107.2	0.49	0.07	0.12	7.62
	127.3	0.58	0.09	0.15	9.16
	144.7	0.66	0.13	0.20	10.58
RC4-3.47-2	107.8	0.49	0.10	0.13	8.11
	135.5	0.62	0.13	0.19	10.47
RC5-0.93-1	32.6	0.47	0.07	0.12	3.92
	39.5	0.57	0.11	0.16	5.22
	46.1	0.67	0.14	0.22	6.25
	53.0	0.77	0.16	0.24	7.47
RC5-0.93-2	36.4	0.53	0.08	0.13	4.25
	43.1	0.62	0.12	0.20	5.63
	52.9	0.77	0.16	0.26	7.48

In view of the main cracks on the reinforced RAMC beams, the frequency histogram of w_i/w_m is exhibited in Figure 5. This basically fits a normal distribution with a variation coefficient of 0.479. With the assurance rate at 95%, the coefficient of the maximum width enlarged for an average $\tau_s = 0.876 + 1.645 \times 0.479 = 1.66$. It is equal to that of the conventional reinforced concrete beams [30,35].

Figure 5. Probability distribution histogram of w_i/w_{cr} .

Form Table 4, the cracking resistance is only 8–34% of the ultimate. This means that the reinforced RAMC beam is always working with cracks under normal service loads. Therefore, the prediction of crack width is necessary. Referencing the specification of China

code GB 50010 [30], the average crack width w_{cr} and the maximum crack width w_{max} can be predicted as follows:

$$w_{cr} = \alpha_c \psi \frac{\sigma_s}{E_s} l_{cr} \quad (9)$$

$$w_{max} = \tau_s w_{cr} \quad (10)$$

$$\psi = 1.1 - \frac{0.65 f_t}{\sigma_s \rho_{te}} \quad (11)$$

$$\sigma_s = \frac{M}{0.87 h_0 A_s} \quad (12)$$

where σ_s is the stress of longitudinal tensile rebars; α_c is the influencing coefficient of concrete between cracks; ψ is the coefficient related to the uneven tensile strain of steel rebar between cracks, taken $\psi = 0.2$ when $\psi < 0.2$, and taken $\psi = 1.0$ when $\psi > 1.0$.

Based on the test data of this study, it is suitable taken $\alpha_c = 0.77$. This is the same with that for conventional referenced concrete beams [30]. The ratios of the test results to the computed values of the w_{cr} and the w_{max} are exhibited in Figure 6. The ratios of w_{cr} changed from 0.701 to 1.440 with an average of 0.988 and a variation coefficient of 0.176. The ratios of the w_{max} changed from 0.765 to 1.268 with an average of 0.991 and a variation coefficient of 0.125.

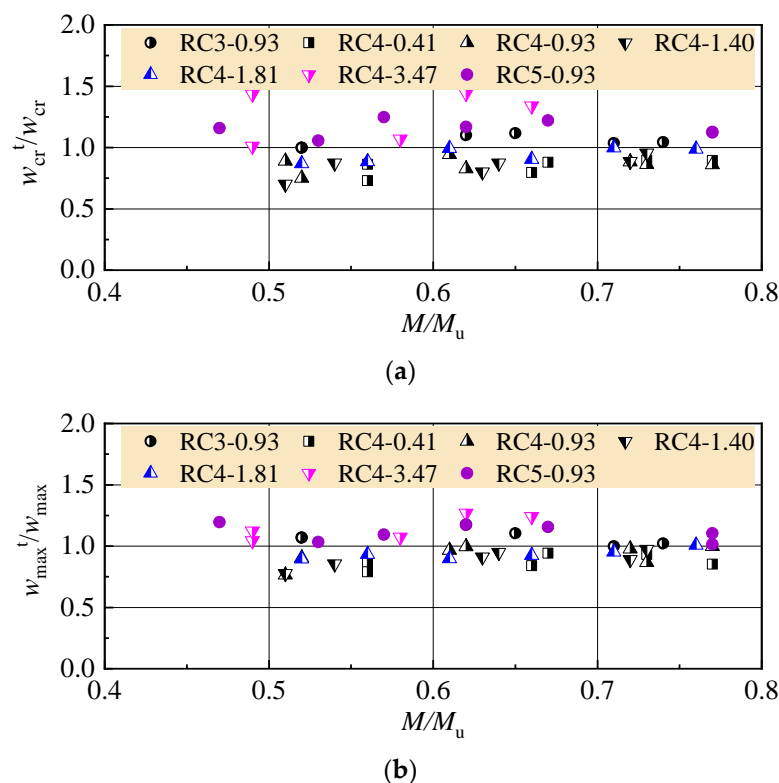


Figure 6. Ratios of test to calculated values: (a) average crack width; (b) maximum crack width.

Combining with the statistical result of average crack spacing, the crack width of reinforced RAMC beams is about 16% larger than that of the conventional reinforced concrete beams.

Meanwhile, the formulas specified in the China codes are also used to evaluate the crack width of test beams. The formulas in DL/T 5057 are [33]:

$$w_{max} = 1.3 \frac{\sigma_s}{E_s} \left(1 - \frac{f_{tk}}{1.4 \sigma_s \rho_{te}} \right) l_{cr} \quad (13)$$

$$l_{cr} = 2.1c + 0.12d/\rho_{te} \quad (14)$$

where the effective reinforcement ratio $\rho_{te} = A_s/2a_sb$, a_s is the distance of harycenter of longitudinal tensile rebars from the edge of cross-section. Taken $\rho_{te} = 0.018$ when $\rho_{te} < 0.018$.

The formula in JTG D62 is [41]:

$$w_{\max} = \frac{\sigma_s}{E_S} \left(\frac{30 + d}{0.28 + 10\rho} \right) \quad (15)$$

The formula in JTJ 267 is [32]:

$$w_{\max} = \frac{\sigma_s}{E_S} \left(\frac{c + d}{0.30 + 1.4\rho_{te}} \right) \quad (16)$$

where the effective reinforcement ratio $\rho_{te} = A_s/2a_sb$, σ_s is the distance of harycenter of longitudinal tensile rebars from the edge of cross-section. Taken $\rho_{te} = 0.018$ when $\rho_{te} < 0.018$, and taken $\rho_{te} = 0.1$ when $\rho_{te} > 0.1$.

With above formulas, the ratio of test result to computed value of the w_{\max} is calculated. For the formulas in DL/T 5057, JTG D62 and JTJ 267. The average ratio is 1.274, 1.086 and 1.163 with a variation coefficient of 0.164, 0.212 and 0.198, respectively. As presented in Figure 7, the computed values of w_{\max} vary within $\pm 30\%$ deviation from the test ones.

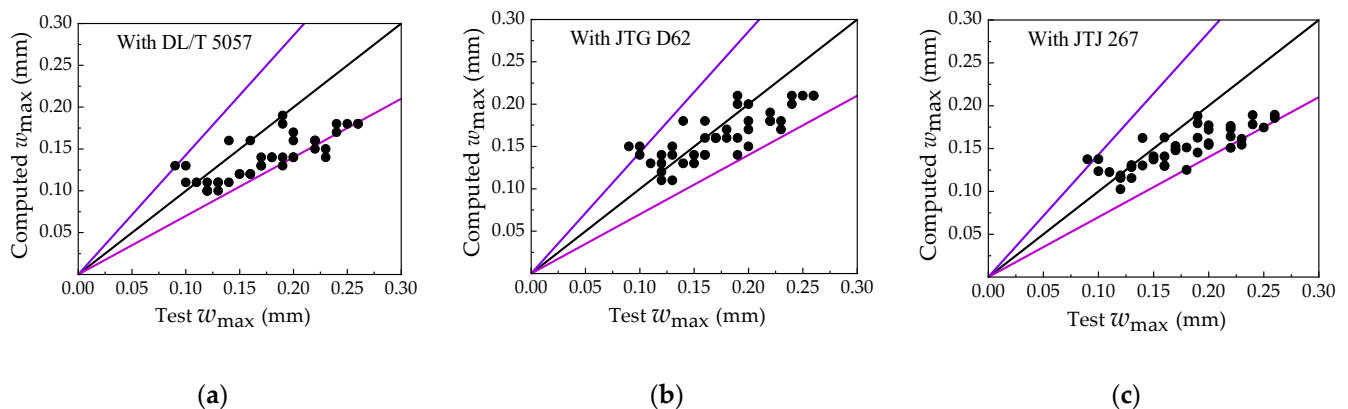


Figure 7. Comparison of test to computed maximum crack width by the formulas specified in codes: (a) DL/T 5057; (b) JTG D62; (c) JTJ 267.

3.4. Mid-span Deflection

As presented in Figure 8, the mid-span deflection curves with the moment load of the test beams consisted of three stages. The first stage was from the initial to the cracking of RAMC. The second one prolonged from the cracking of RAMC to the yield of tensile rebars with the continuously decreased slope of the ascending curve owing to the generation and extension of cracks. The plasticity of RAMC in compression zone becomes obvious with the increase in reinforcement ratio. The flexural stiffness becomes lower, especially at the segment closed to the yield of tensile rebars. The third stage was almost a flat segment with a large increment of the deflection under a lower decrease in loads, which presents an ideal ductility of test beams under static load. At the same time, the curves of test beams with different strength of RAMC almost overlapped. This presents that the strength of RAMC has little effect of on the deflection.

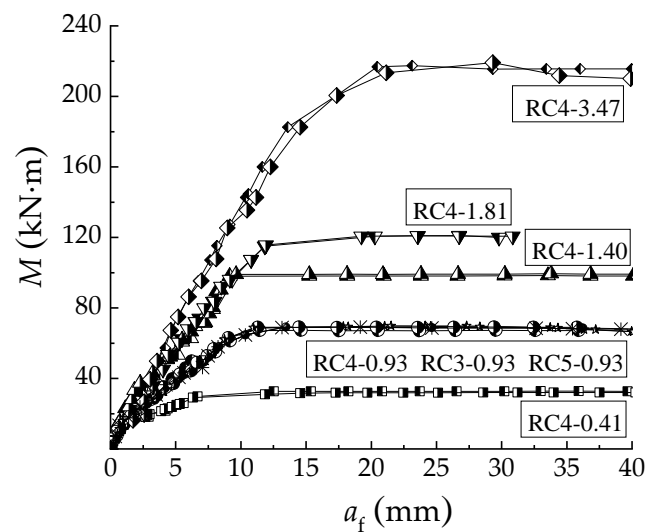


Figure 8. Mid-span deflection vs moment curves of test beams.

With the assumption of a uniform flexural stiffness along the span of beams, the following formula can be applied to compute the mid-span deflections of the reinforced RAMC beams:

$$a_f = 0.1132M \cdot l_0^2 / B_s \quad (17)$$

where B_s is the equivalent flexural stiffness of beam.

With the tested a_f at the normal serviceability in Table 5, the tested flexural stiffness B_s^t can be computed with the formula; values are presented in Figure 9. Corresponding to the increase of a_f^t , B_s^t decreased with the increasing load level M/M_u . The increase in the reinforcement ratio contributed obviously to the B_s^t , while the strength of RAMC had little influence on the B_s^t .

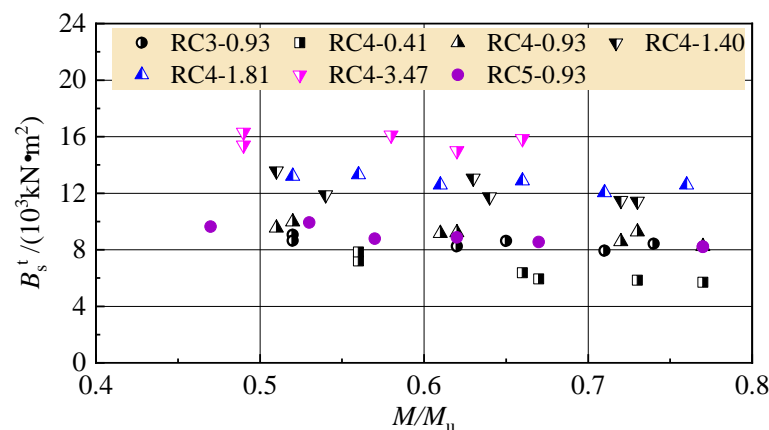


Figure 9. Flexural stiffness changed with moment of the test beams.

Referring the conventional reinforced concrete beams, the following formula is used for the computation of equivalent flexural stiffness of reinforced RAMC beams [30]:

$$B_s = \frac{E_s A_s h_0^2}{1.15\psi + 0.2 + 6\alpha_E \rho} \quad (18)$$

where α_E is the ratio of the modulus of elasticity, $\alpha_E = E_s / E_c$.

The ratios of the tested to calculated flexural stiffness B_s^t / B_s , as displayed in Figure 10, changed from 0.762 to 1.067 with an average of 0.905 and a variation coefficient of 0.081. This indicates a decrement of about 10% of the flexural stiffness of test beams compared

with those predicted by the formula for the conventional concrete beams. The main reason could be due to a larger crack width on test beams, and a decreased modulus of elasticity of RAMC. As presented in Table 3, the test values of the modulus of elasticity decreased by about 3% compared with those predicted by the formula of conventional concrete [30].

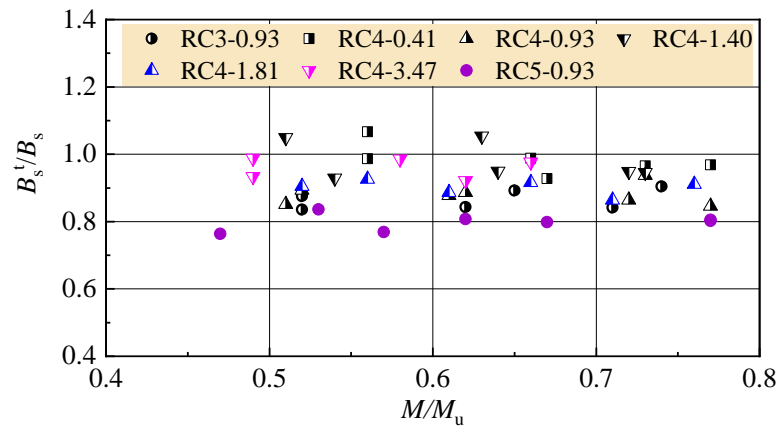


Figure 10. Ratios of test to computed flexural stiffness.

With above formulas, the ratio of the test results to the computed values of the mid-span deflection of test beams at normal serviceability was calculated. The ratios vary from 0.937 to 1.310, as presented in Figure 11. The average was 1.112 with a variation coefficient of 0.081. About a 10% increment of the mid-span deflection took place on test beams due to the decrease in the flexural stiffness. This indicates that an unsafe result with a small predicted mid-span deflection can be attained from the formulas specified in the China code GB 50,010 [30].

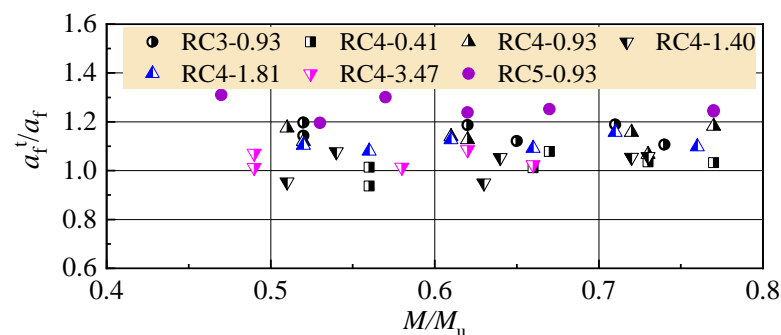


Figure 11. Ratios of test to computed values of mid-span deflection.

4. Conclusions

(1) On the premise of the longitudinal tensile rebars yielded before the crushing of RAMC in compression, the reinforced RAMC beams had the same bearing capacity under bending compared to that of the conventional reinforced concrete beams. The same formulas can be used to calculate the ultimate moment at bearing capacity;

(2) The cracking resistance of reinforced RAMC beams is about 20% lower than that of conventional reinforced concrete beams. This leads to an issue of the reinforced RAMC beams with cracks at normal serviceability, owing to the cracking moment being only 8–34% of the ultimate moment;

(3) With the changes of the reinforcement ratio and strength of RAMC, reinforced RAMC beams presented similar changes of the crack width and deflection to those predicted by the formulas for the conventional reinforced concrete beams. However, the crack width and deflection of reinforced RAMC beam increased by about 16 and 10% compared with the predicted ones;

(4) The poor serviceability of reinforced RAMC beam comes inherently from a lower tensile strength of RAMC and a weakened bond strength of rebar. Therefore, the improvement of mechanical properties of RAMC, especially the strengthening of tensile strength, is still a basic issue to be studied further.

Author Contributions: Methodology, C.L., Y.Y. and X.Z.; validation, S.Z.; formal analysis, T.L.; investigation, C.L., T.L. and H.F.; data curation, C.L.; writing—original draft preparation, T.L., H.F. and X.Z.; writing—review and editing, Y.Y. and C.L.; supervision, S.Z.; funding acquisition, X.Z. and S.Z. All authors have read and agreed to the published version of the manuscript.

Funding: This research was funded by the “Natural Science Foundation of Henan, China, grant number 202102310250”; “Key Scientific and Technological Research Project of University in Henan, China, grant number 20A560014”.

Institutional Review Board Statement: Not applicable.

Informed Consent Statement: Not applicable.

Data Availability Statement: The data presented in this study are available on request from the corresponding author.

Conflicts of Interest: The authors declare no conflict of interest.

References

1. Ministry of Housing and Urban-Rural Construction of the People’s Republic of China. *Technique Specification for Application of Recycled Aggregate*; JGJ/T 240-2011; China Building Industry Press: Beijing, China, 2011.
2. Xiao, J.Z.; Li, W.G.; Fan, Y.H. An overview of study on recycled aggregate concrete in China. *Constr. Build. Mater.* **2012**, *31*, 364–383. [[CrossRef](#)]
3. Ministry of Housing and Urban-Rural Construction of the People’s Republic of China. *Technique Specification for Application of Manufactured Sand Concrete*; JGJ/T 241-2011; China Building Industry Press: Beijing, China, 2011.
4. Li, F.L.; Liu, C.J.; Pan, L.Y.; Li, C.Y. *Manufactured Sand Concrete*; China Waterpower Press: Beijing, China, 2014.
5. Hendriks, C.F.; Pietersen, H.S. *Sustainable Raw Materials: Construction and Demolition Waste—State-of-the-Art Report of RILEM Technical Committee 165-SRM*; RILEM Publications: Geneva, Switzerland, 2000.
6. Butler, L.; West, J.S.; Tighe, S.L. Effect of recycled concrete coarse aggregate from multiple sources on the hardened properties of concrete with equivalent compressive strength. *Constr. Build. Mater.* **2013**, *47*, 1292–1301. [[CrossRef](#)]
7. Lotfi, S.; Eggimann, M.; Wagner, E. Performance of recycled aggregate concrete based on a new concrete recycling technology. *Constr. Build. Mater.* **2015**, *95*, 243–256. [[CrossRef](#)]
8. Santos, S.A.; Da Silva, P.R.; De Brito, J. Mechanical performance evaluation of self-compacting concrete with fine and coarse recycled aggregates from the precast industry. *Material* **2017**, *8*, 904. [[CrossRef](#)]
9. Seo, D.S.; Choi, H.B. Effects of the old cement mortar attached to the recycled aggregate surface on the bond characteristics between aggregate and cement mortar. *Constr. Build. Mater.* **2014**, *59*, 72–77. [[CrossRef](#)]
10. Sidorova, A.; Vazquez-Ramonich, E.; Barra-Bizinotto, M. Study of the recycled aggregates natures influence on the aggregate cement paste interface and ITZ. *Constr. Build. Mater.* **2014**, *68*, 677. [[CrossRef](#)]
11. Butler, L.; West, J.S.; Tighe, S.L. Bond of reinforcement in concrete incorporating recycled concrete aggregates. *J. Struct. Eng.* **2015**, *141*, B4014001. [[CrossRef](#)]
12. Aseel, A.; Raad, A.; Hussein, A. Bond strength behavior for deformed steel rebar embedded in recycled aggregate concrete. *J. Eng. Technol. Sci.* **2021**, *53*, 1–18.
13. Seara-Paz, S.; González-Fontebona, B.; Martínez-Abella, F.; Carro-López, D. Long-term flexural performance of reinforced concrete beams with recycled coarse aggregates. *Constr. Build. Mater.* **2018**, *176*, 593–607. [[CrossRef](#)]
14. Arezoumandi, M.; Smith, A.; Volz, J.S.; Khayat, K.H. An experimental study on flexural strength of reinforced concrete beams with 100% recycled concrete aggregate. *Eng. Struct.* **2015**, *88*, 154–162. [[CrossRef](#)]
15. Rahal, K.N.; Alrefaei, Y.T. Shear strength of longitudinally reinforced recycled aggregate concrete beams. *Eng. Struct.* **2017**, *145*, 273–282. [[CrossRef](#)]
16. Chaboki, H.R.; Ghalehnovi, M.; Karimipour, A.; de Brito, J. Experimental study on the flexural behaviour and ductility ratio of steel fibres coarse recycled aggregate concrete beams. *Constr. Build. Mater.* **2018**, *186*, 400–422. [[CrossRef](#)]
17. Chaboki, H.R.; Ghalehnovi, M.; Karimipour, A.; de Brito, J.; Khatibini, M. Shear behaviour of concrete beams with recycled aggregate and steel fibres. *Constr. Build. Mater.* **2019**, *204*, 809–827. [[CrossRef](#)]
18. Ghoneim, M.; Yehia, A.; Yehia, S.; Abuzaid, W. Shear strength of fiber reinforced recycled aggregate concrete. *Materials* **2020**, *13*, 4183. [[CrossRef](#)]
19. Li, C.Y.; Wang, F.; Deng, X.S.; Li, Y.Z.; Zhao, S.B. Testing and prediction of the strength development of recycled-aggregate concrete with large particle natural aggregate. *Materials* **2019**, *12*, 1891. [[CrossRef](#)]

20. Li, X.K.; Pei, S.W.; Fan, K.P.; Geng, H.B.; Li, F.L. Bending performance of SFRC beams based on composite-recycled aggregate and matched with 500MPa rebars. *Materials* **2020**, *13*, 930. [[CrossRef](#)]
21. Li, C.Y.; Liang, N.; Zhao, M.L.; Yao, K.Q.; Li, J.; Li, X.K. Shear performance of reinforced concrete beams affected by satisfactory composite-recycled aggregates. *Materials* **2020**, *13*, 1711. [[CrossRef](#)] [[PubMed](#)]
22. Bonavetti, V.L.; Irassar, E.F. The effect of stone dust content in sand. *Cem. Concr. Res.* **1994**, *24*, 580–590. [[CrossRef](#)]
23. Kakali, G.; Tsivilis, S.; Aggeli, E.; Bali, M. Hydration Prod. of C₃A, C₃S and Portland cement in the presence of CaCO₃. *Cem. Concr. Res.* **2000**, *30*, 1073–1077. [[CrossRef](#)]
24. Ding, X.X.; Li, C.Y.; Xu, Y.Y.; Li, F.L.; Zhao, S.B. Experimental study on long-term compressive strength of concrete with manufactured sand. *Constr. Build. Mater.* **2016**, *108*, 67–73. [[CrossRef](#)]
25. Zhao, S.B.; Ding, X.X.; Zhao, M.S.; Li, C.Y.; Pei, S.W. Experimental study on tensile strength development of concrete with manufactured sand. *Constr. Build. Mater.* **2017**, *138*, 247–253. [[CrossRef](#)]
26. Zhao, S.B.; Ding, X.X.; Li, C.M.; Li, C.Y. Experimental study of bond properties between deformed steel bar and concrete with machine-made sand. *J. Build. Mater.* **2013**, *16*, 191–196. [[CrossRef](#)]
27. Zhao, S.B.; Guo, Q.; Li, G.X.; Su, Y.F.; Shao, W.J. Basic mechanical properties of concrete with machine-made sand and recycled coarse aggregate. *Appl. Mechan. Mater.* **2013**, 357–360, 1102–1105. [[CrossRef](#)]
28. General Administration of Quality Supervision, Inspection and Quarantine of the People's Republic of China. *Common Portland Cement*; GB 175-2007; China Standard Press: Beijing, China, 2007.
29. Ministry of Housing and Urban-Rural Construction of the People's Republic of China. *Standard of Test Methods of Concrete Structures*; GB/T50152-2012; China Building Industry Press: Beijing, China, 2012.
30. Ministry of Housing and Urban-Rural Construction of the People's Republic of China. *Code for Design of Concrete Structures*; GB50010-2010; China Building Industry Press: Beijing, China, 2010.
31. Pan, L.Y.; Shao, W.J.; Li, G.X.; Li, H.F. Experimental study on flexural resistance of reinforced recycled-concrete beams. *Appl. Mechan. Mater.* **2013**, 438–439, 789–793. [[CrossRef](#)]
32. Ministry of Transport of the People's Republic of China. *Code for Design of Concrete Structures in Port Engineering*; JTJ 267-98; China People's Transport Press: Beijing, China, 1998.
33. General Administration of Quality Supervision, Inspection and Quarantine of the People's Republic of China. *Code for Design of Hydraulic Concrete Structures*; DL/T5057-2009; China Power Press: Beijing, China, 2009.
34. Zhao, S.B.; Shao, W.J.; Li, C.Y. Experimental study on cracking resistance of normal section of reinforced MSRCAC beams. *J. North China Univ. Water Resour. Electric Power* **2013**, *34*, 46–49.
35. Zhao, S.B.; Guan, J.F.; Chen, X.T.; Zhang, X.P. Experimental research on similitude ratio of resistance against cracking of normal section of reinforced concrete flexural members. *J. Yangtze River Sci. Res. Inst.* **2007**, *24*, 64–71.
36. Zhao, S.B.; Guan, J.F.; Chen, X.T.; Zhang, X.P.; Huang, C.K. Experimental studies and statistical analysis of crack patterns of reinforced concrete beams. *Eng. Mechan.* **2008**, *25*, 141–146.
37. Li, C.Y.; Zhao, M.L.; Ren, F.C.; Liang, N.; Li, J.; Zhao, M.S. Bond properties between full-recycled-aggregate concrete and deformed steel bar. *Open Civ. Eng. J.* **2017**, *11*, 685–698. [[CrossRef](#)]
38. Seara-Paz, S.; González-Fontebo, B.; Eiras-López, J.; Herrador, M.F. Bond behavior between steel reinforcement and recycled concrete. *Mater. Struct.* **2014**, *47*, 323–334. [[CrossRef](#)]
39. Zhao, M.S.; Li, C.Y.; Su, J.Z.; Shang, P.R.; Zhao, S.B. Experimental study and theoretical prediction of flexural behaviors of reinforced SFRELC beams. *Constr. Build. Mater.* **2019**, *208*, 454–463. [[CrossRef](#)]
40. Ministry of Housing and Urban-Rural Construction of the People's Republic of China. *Code for Durability Design of Concrete Structures*; GB50476-2019; China Building Industry Press: Beijing, China, 2019.
41. Ministry of Transport of the People's Republic of China. *Code for Design of Reinforced Concrete and Prestressed Concrete Highway Bridge and Culvert*; JTG D62-2004; China People's Transport Press: Beijing, China, 2004.